Journal of Molecular Structure: THEOCHEM 900 (2009) 84–89

Contents lists available at ScienceDirect

Journal of Molecular Structure: THEOCHEM

journal homepage: www.elsevier.com/locate/theochem

First-principles study of crystalline mono-amino-2,4,6-trinitrobenzene, 1,3-diamino-2,4,6-trinitrobenzene, and 1,3,5-triamino-2,4,6-trinitrobenzene

Weihua Zhu *, Xiaowen Zhang, Tao Wei, Heming Xiao *

Institute for Computation in Molecular and Materials Science and Department of Chemistry, Nanjing University of Science and Technology, Nanjing 210094, China

ARTICLE INFO

Article history:
Received 27 November 2008
Received in revised form 20 December 2008
Accepted 20 December 2008
Available online 29 December 2008

Keywords:
Density functional theory
Density of states
Band gap
Thermodynamic properties

ABSTRACT

The electronic structure and thermodynamic properties of crystalline mono-amino-2,4,6-trinitrobenzene (MATB), 1,3-diamino-2,4,6-trinitrobenzene (DATB), and 1,3,5-triamino-2,4,6-trinitrobenzene (TATB) have been comparatively studied using density functional theory in the local density approximation. An analysis of electronic structure shows that the C—NO_2 bonds in the three solids are easier to be broken in the thermal decomposition than the C—NH_2 bonds. The calculated thermodynamic properties show that the order of their thermodynamic stability is TATB > DATB > MATB and their decomposition reactions are favorable under high temperature. Finally, an attempt is made to correlate the impact sensitivity of the three solids with their band gap. The result shows that there is the relationship between the band gap and impact sensitivity.

1. Introduction

Solid energetic nitro compounds have long played an important technological role as explosives and as fuels. Over the past several decades a large number of studies have been devoted to their structure, properties, and decomposition mechanism [1–3]. Among them, the compounds mono-amino-2,4,6-trinitrobenzene (MATB), 1,3-diamino-2,4,6-trinitrobenzene (DATB), and 1,3,5-triamino-2,4,6-trinitrobenzene (TATB) are a category of explosives and their molecular properties, sensitivity to various stimuli, and explosive performance are extensively investigated and compared [4–15]. Unfortunately, many fundamental and practical problems of these compounds are still not well understood because they possess a complex chemical behavior. In the series of crystalline MATB, DATB, and TATB, there is a variation in the stability to impact and shock. Therefore, understanding the differences between the structure and fundamental properties of the three solids is important for the development of new energetic materials.

A desire to probe more fundamental questions relating to the basic properties of these solids as energetic materials is generating significant interest in the basic solid-state properties of such energetic systems. The electronic structure is intimately related to their fundamental physical and chemical properties; moreover, an understanding of electronic structure and properties is necessary for discussion of electronic processes as they relate to decomposition and initiation. On the other hand, although the detailed decomposition mechanism by which the solids releases energy under mechanical shock is still not well understood, it has been suggested that their decomposition may result from transferring thermal and mechanical energy into the internal degrees of freedom of tightly bonded groups of atoms in solids [16–18]. Therefore, the knowledge of their electronic and thermodynamic properties appears to be very important in understanding their explosive properties.

The investigation of the microscopic properties of energetic materials, which possess a complex chemical behavior, remains to be a challenging task. Theoretical calculations are an effective way to model the physical and chemical properties of complex solids at the atomic level as a complement to experimental work. As the electronic structure and thermodynamic properties of the three solid are not systematically investigated and compared, there is a clear need to gain an understanding of those at the ab initio level.

In this study we performed periodic density functional theory (DFT) calculations to study the electronic structure and thermodynamic properties of crystalline MATB, DATB, and TATB. Our main purpose here is to examine the differences in the electronic structure and properties among them.

The remainder of this paper is organized as follows. A brief description of our computational method is given in Section 2. The results and discussion are presented in Section 3, followed by a summary of our conclusions in Section 4.

2. Computational method

The calculations performed in this study were done using the CASTEP code [19] based on DFT with Vanderbilt-type ultrasoft

* Corresponding authors. Fax: +86 25 84303919.
E-mail addresses: zhuwh@mail.njust.edu.cn (W. Zhu), xiao@mail.njust.edu.cn (H. Xiao).

0166-1280/$ - see front matter © 2008 Elsevier B.V. All rights reserved.
doi:10.1016/j.theochem.2008.12.031

pseudopotentials [20] and a plane-wave expansion of the wave functions. The self-consistent ground state of the system was determined by using a band-by-band conjugate gradient technique to minimize the total energy of the system with respect to the plane-wave coefficients. The electronic wave functions were obtained by a density-mixing scheme [21] and the structures were relaxed by using the Broyden, Fletcher, Goldfarb, and Shannon (BFGS) method [22]. The local density approximation (LDA) functional proposed by Ceperley and Alder [23] and parameterized by Perdew and Zunger [24] named CA–PZ, was employed. The cutoff energy of plane-waves was set to 400.0 eV. Brillouin zone sampling was performed by using the Monkhost–Pack scheme with a *k*-point grid of $3 \times 2 \times 1$, $3 \times 3 \times 2$, and $3 \times 3 \times 3$ for MATB, DATB, and TATB, respectively. The values of the kinetic energy cutoff and the *k*-point grid were determined to ensure the convergence of total energies.

MATB crystallizes in a monoclinic $P2_1/c$ space group and contains four molecules per unit cell [25]. DATB crystallizes in a monoclinic space group, *Pc*, with two molecules per unit cell [26]. TATB crystallizes in a triclinic space group, $P\bar{1}$, with two molecules per unit cell [27]. There is strong intramolecular hydrogen bonding involving hydrogen atoms of amino groups with the oxygen atoms of nitro groups in the three solids. Fig. 1 displays the unit cells of the three crystals, and conformations and atomic numberings of molecules in the solid phases are shown in Fig. 2.

Starting from the above-mentioned experimental structures, the geometry relaxation was performed to allow the ionic configurations, cell shape, and volume to change. In the geometry relaxation, the total energy of the system was converged less than 2.0×10^{-5} eV, the residual force less than 0.05 eV/Å, the displacement of atoms less than 0.002 Å, and the residual bulk stress less than 0.1 GPa. For all the relaxed structures, the Mulliken charges and bond populations were investigated using a projection of the plane-wave states onto a linear combination of atomic orbitals (LCAO) basis set [28,29], which is widely used to perform charge transfers and populations analysis. The phonon frequencies at the gamma point have been calculated from the response to small atomic displacements [30].

3. Results and discussion

3.1. Bulk properties

In our previous study [31] we applied three different functionals: LDA (CA–PZ) and generalized gradient approximation (GGA) (PBE [32] and PW91 [33]), to crystalline octahydro-1,3,5,7-tetranitro-1,3,5,7-tetrazocine (HMX) as a test and found that the LDA may be expected to produce more reliable predictions of the structures. Therefore, LDA was used in all calculations here. The calculated cell parameters, bond lengths, and bond angles of crystalline MATB,

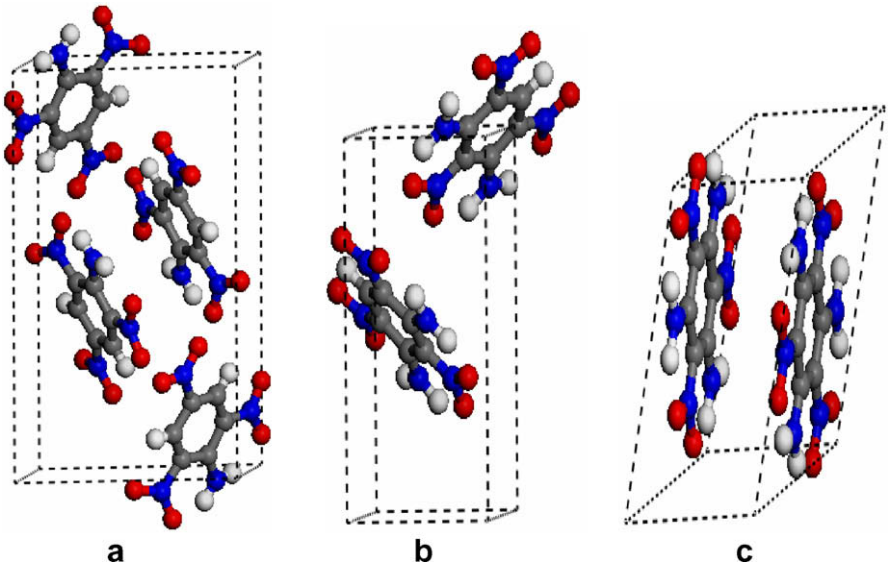

Fig. 1. Unit cells for (a) MATB, (b) DATB, and (c) TATB crystals.

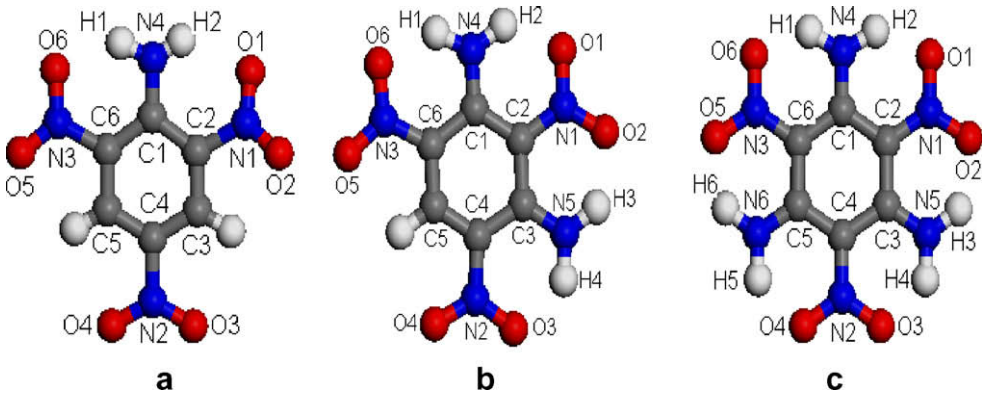

Fig. 2. Conformations and atomic numberings of (a) MATB, (b) DATB, and (c) TATB molecules.

DATB, and TATB are given in Table 1 together with their experimental results. The calculated results reproduce the measured cell parameters of the three solids. The differences between the calculated and experimental values are typical for the LDA approximation to DFT. We also note that the calculated bond lengths and bond angles are very close to the corresponding experimental data except the N–O bond lengths. These discrepancies between the calculated and experimental N–O bond lengths may be due to intermolecular hydrogen bonding interactions present in the crystal lattice, which are not well described by DFT. These comparisons confirm that our computational parameters are reasonably satisfactory.

3.2. Electronic structure

The calculated total density of states (DOS) and partial DOS (PDOS) for crystalline MATB, DATB, and TATB are displayed in Figs. 3–5, respectively. Clearly, the structures are very similar except some subtle differences. The DOS of the three solids are finite at the Fermi energy level. This is because the DOS contain some form of broadening effect. In the upper valence band, the three solids have a sharp peak near the Fermi level. The top of the DOS valence band shows five main peaks for MATB, four main peaks for DATB, and four main peaks for TATB. These peaks are predominately from the p states. After that, several main peaks in the upper valence band are superimposed by the s and p states. The conduction band is dominated by the p states. This indicates that the p states for the three solids play a very important role in their chemical reaction. Note that several DOS peaks in the upper valence band merge together, showing that there is good electronic delocalization in the systems. This is because the bonding in the ring is formally aromatic.

The atom-resolved DOS and PDOS of crystalline MATB, DATB, and TATB are also shown in Figs. 3–5, respectively. The main features can be summarized as follows. (i) In the upper valence band, the PDOS of the states of N of amino groups and C are far larger than that of the states of N of nitro groups. It is expected that the states of N of amino groups and C make more important con-

Table 1
Experimental and relaxed cell parameters, bond lengths (Å), and bond angles (deg) for crystalline MATB, DATB, and TATB.

	MATB		DATB		TATB	
	This work	Expt [27]	This work	Expt [28]	This work	Expt [29]
Cell parameter						
a (Å)	6.0879	6.137	6.9737	7.300	9.0022	9.010
b (Å)	9.3739	9.217	5.8432	5.200	9.0111	9.028
c (Å)	15.3779	15.323	11.3116	11.630	6.7917	6.812
α (deg)					104.408	108.590
β (deg)	99.672	99.670	89.901	99.900	92.873	91.820
γ(deg)					119.935	119.970
Bond length						
C1–C2	1.435	1.428	1.466	1.472	1.437	1.430
C2–C3	1.369	1.376	1.456	1.467	1.438	1.430
C3–C4	1.384	1.372	1.473	1.386	1.437	1.434
C4–C5	1.378	1.380	1.372	1.375	1.437	1.433
C5–C6	1.375	1.372	1.368	1.379	1.436	1.433
C6–C1	1.437	1.429	1.474	1.392	1.435	1.435
N1–C2	1.432	1.463	1.398	1.415	1.395	1.401
N2–C4	1.426	1.469	1.502	1.514	1.394	1.399
N3–C6	1.427	1.475	1.418	1.438	1.397	1.401
N4–C1	1.319	1.340	1.315	1.317	1.317	1.314
N5–C3			1.317	1.323	1.314	1.312
N6–C5					1.314	1.313
N1–O1	1.253	1.230	1.263	1.242	1.274	1.269
N1–O2	1.247	1.202	1.267	1.262	1.267	1.272
N2–O3	1.250	1.222	1.264	1.235	1.273	1.271
N2–O4	1.249	1.224	1.255	1.177	1.269	1.273
N3–O5	1.243	1.215	1.251	1.223	1.272	1.268
N3–O6	1.265	1.219	1.261	1.259	1.267	1.275
Bond angle						
C1–C2–C3	122.7	123.7	121.9	120.5	121.0	120.6
C2–C3–C4	119.1	118.5	116.7	116.7	118.8	119.1
C3–C4–C5	121.6	122.4	120.7	124.0	121.0	120.8
C4–C5–C6	119.4	117.7	122.6	119.2	118.9	118.9
C5–C6–C1	122.2	124.4	120.8	123.8	121.0	120.6
C6–C1–C2	114.7	112.9	116.8	115.8	118.9	119.3
C1–C2–N1	120.5	121.1	118.8	119.8	119.5	119.5
C2–N1–O1	118.3	118.7	120.7	120.8	121.2	121.4
C2–N1–O2	118.1	118.9	120.7	121.8	121.4	121.2
O1–N1–O2	123.4	122.2	118.5	117.2	117.3	117.2
C3–C4–N2	119.2	118.8	122.5	121.9	119.5	119.4
C4–N2–O3	117.7	117.6	119.8	115.5	121.3	121.5
C4–N2–O4	118.5	117.8	119.1	117.7	121.4	121.3
O3–N2–O4	123.6	124.5	121.0	126.6	117.2	117.0
C5–C6–N3	116.4	115.7	116.3	113.6	119.5	119.4
C6–N3–O5	119.4	117.3	119.0	121.1	121.3	121.6
C6–N3–O6	118.1	118.7	119.8	118.7	121.3	121.0
O5–N3–O6	122.3	123.9	121.0	120.0	117.3	117.3
N4–C1–C2	122.5	123.7	122.7	120.1	120.6	120.3
N5–C3–C4			120.5	124.0	120.7	120.1
N6–C5–C6					120.4	120.2

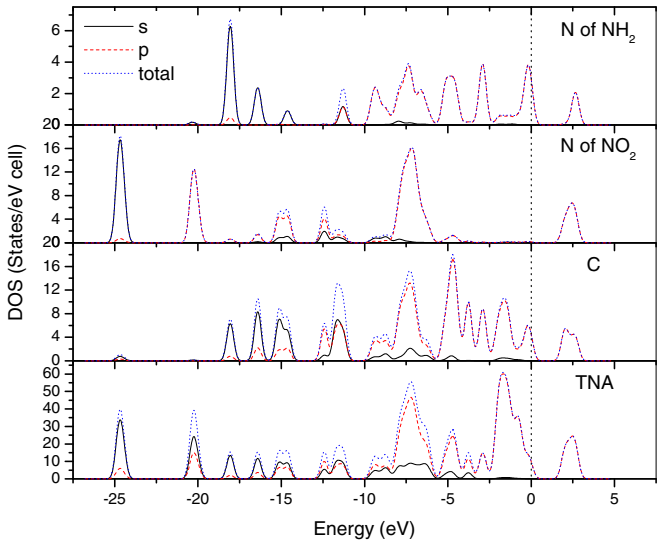

Fig. 3. Total and partial density of states (DOS) of N-states, O-states of OH, C-states, and MATB. The Fermi energy is shown as a dashed vertical line.

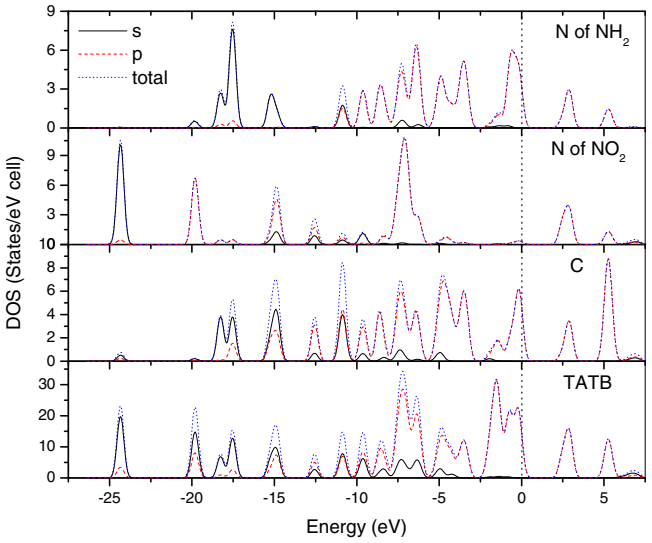

Fig. 5. Total and partial density of states (DOS) of N-states, O-states of OH, C-states, and TATB.

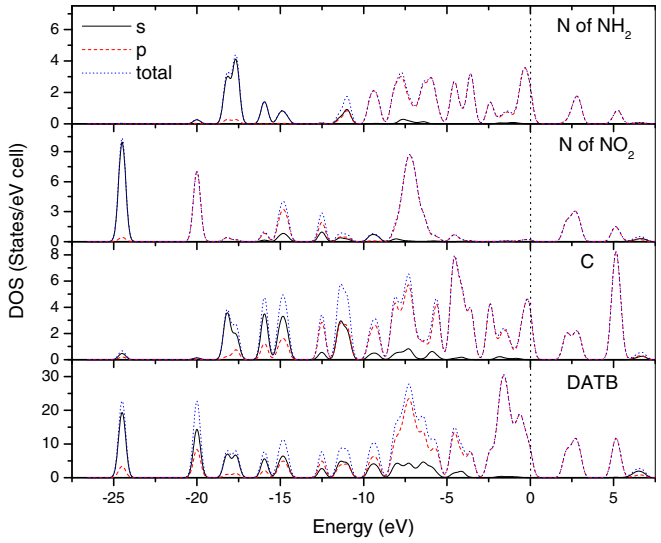

Fig. 4. Total and partial density of states (DOS) of N-states, O-states of OH, C-states, and DATB.

tributions to the valence bands than these of nitro groups. This shows that N in amino group acts as an active center. (ii) For MATB, some strong peaks occur at the same energy in the PDOS of a particular C atom and a particular N atom of amino groups. It can be inferred that the two atoms are strongly bonded. Similarly, a particular N atom of nitro groups and a particular C atom are strongly bonded. The same is true of DATB and TATB. (iii) There are some differences in the PDOS of the N atoms of nitro groups for the three solids. This is due to the differences in their local molecular packing. The same is true of the C atoms. (iv) In the conduction band region of DOS, the peaks of the three solids are dominated by the C-p states and N-p states. (v) In the energy range from −5.0 to 0 eV, the DOS of the three solids are superimposed by the C-states and N-states of amino groups, while the contribution from the N-states of nitro groups to the total DOS is very small. It may be inferred that the C–NO_2 bonds in the three solids may be firstly broken in the thermal decomposition. This is agreement with the previous experimental report [5].

The electronic structure can be further analyzed by examining the charge transfer and bond order in the three solids. The Mulliken charge and overlap population are useful in evaluating the nature of bonds in a compound. Although the absolute magnitudes of Mulliken populations have little physical meaning, the relative values can still offer some useful information. Table 2 shows the atomic charge and bond order values for crystalline MATB, DATB, and TATB. When the H atom in the ring is substituted by amino group, the atomic charge of its adjacent C atom becomes positive. In TATB all the atomic charges of C are positive. This shows that TATB is the most stable of the three solids. The atomic charge of N1 of nitro group in the three solids is in the following order: MATB > DATB > TATB. The same is true of N2 and N3 of nitro groups. This is because nitro groups in TATB have adjacent amino groups and form six intramolecular hydrogen bonds, whereas there are two and four hydrogen bonds for MATB and DATB, respectively. The atomic charges of the O atoms of nitro groups in the three solids are different, reflecting that the nitro groups are in different local packing. The atomic charges of N atoms of NH_2 groups in the three solids are different. This is due to strong intramolecular hydrogen bonding between the nitro and amino groups.

Bond order is a measure of the overall bond strength between two atoms. A high value of the bond order indicates a covalent bond, while a low value shows an ionic nature. The bond orders of the C–C bonds are from 1.02 to 1.15 in MATB. This is due to the influence of the different substituents in the benzene ring. Therefore, the bond orders are affected by the presence of other nearby atoms, not just the two atoms that form a bond. The same is true of the C–C bonds in DATB. But the bond orders of the C–C bonds in TATB are almost equal. This is because the substituents in TATB are in symmetric position. The bond order of the N1–C2 bonds in the three solids is in the following order: MATB < DATB < -TATB. This shows that intramolecular hydrogen bonding between the nitro and amino groups make the N1–C2 bonds become strong. The same is true of the N2–C4 and N3–C6 bonds. From these discussions, one may infer that the stability for this series increases in the following sequence: MATB < DATB < TATB, which is in agreement with their experimental order [5]. The bond orders of the N1–O1 and N1–O2 bonds are not equal in the three solids, reflecting the two bonds are in different local packing. The same is true of other N–O bonds. The bond order of the C–NH_2 bonds in the three solids increases in the following order: MATB < DATB < TATB.

Table 2
Calculated atomic charges (e) and bond orders for crystalline MATB, DATB, and TATB.

	MATB	DATB	TATB
Atomic charge			
C1	0.19	0.21	0.19
C2	0.08	0.07	0.07
C3	−0.21	0.20	0.20
C4	0.10	0.08	0.06
C5	−0.23	−0.20	0.19
C6	0.09	0.09	0.06
N1	0.39	0.36	0.35
N2	0.40	0.37	0.35
N3	0.39	0.39	0.35
O1	−0.41	−0.40	−0.40
O2	−0.34	−0.41	−0.42
O3	−0.36	−0.40	−0.41
O4	−0.38	−0.40	−0.43
O5	−0.36	−0.39	−0.40
O6	−0.36	−0.39	−0.43
N4	−0.73	−0.72	−0.72
N5		−0.72	−0.71
N6			−0.71
Bond order			
C1–C2	1.02	1.04	1.02
C2–C3	1.13	1.04	1.02
C3–C4	1.08	0.99	1.01
C4–C5	1.06	1.11	1.02
C5–C6	1.15	1.13	1.02
C6–C1	1.02	0.99	1.02
N1–C2	0.76	0.85	0.88
N2–C4	0.73	0.80	0.89
N3–C6	0.74	0.79	0.88
N1–O1	0.68	0.69	0.69
N1–O2	0.76	0.68	0.68
N2–O3	0.74	0.69	0.68
N2–O4	0.73	0.73	0.67
N3–O5	0.74	0.74	0.69
N4–O6	0.71	0.70	0.67
N4–C1	1.01	1.01	1.02
N5–C3		1.01	1.03
N6–C5			1.03

3.3. Thermodynamic properties

In this section the thermodynamic functions including entropy, heat capacity, enthalpy, and free energy for crystalline MATB, DATB, and TATB are evaluated and presented in Fig. 6. With the increase of temperature, the calculated entropies of the three solids monotonically increase. This is because the main contributions to the entropy are from the translations and rotations of the molecules at lower temperature, whereas the vibrational motion is intensified at higher temperature and makes more contributions to the entropy. Note that the entropy for the three solids increases in the following order: DATB < TATB < MATB with the increase of temperature. The same is true of the enthalpy and heat capacity. For the free energy, the case is quite the contrary. As the temperature increases, the free energy values of the three solids gradually decrease; moreover, their decreasing order is as follows: MATB > TATB > DATB.

Based on the calculated thermodynamic functions, the enthalpy of formation and the free energy of formation can be evaluated. Concerning the formation energy, we consider the stabilities of the three solids with respect to decomposition reactions (1)–(3), respectively.

$$C_6H_4N_4O_6 \rightarrow 2HCN + 2CO_2 + 2CO + H_2 + N_2 \quad (1)$$

$$C_6H_5N_5O_6 \rightarrow 2HCN + 2CO_2 + 2CO + 3/2H_2 + 3/2N_2 \quad (2)$$

$$C_6H_6N_6O_6 \rightarrow 2HCN + 2CO_2 + 2CO + 2H_2 + 2N_2 \quad (3)$$

The calculated enthalpy and free energy of formation for the three solids are shown in Figs. 7 and 8, respectively. It can be seen that the enthalpies of formation for the three solids become more and more positive with increasing temperature. This shows that the primary fission reactions are exothermic. As the temperature increases, the enthalpy of formation for the three solids increases in the following order: MATB < DATB < TATB. It is found from Fig. 8 that the free energies of formation for the three solids are negative in the whole temperature range; moreover, the free energy of formation for the three solids decreases in the following order: MATB > DATB > TATB. This shows that the decomposition reactions (1)–(3) are thermodynamically favorable under high temperature; moreover, their thermal stability increases in the following order: MATB < DATB < TATB.

3.4. Correlation of band gap with impact sensitivity

In this section an attempt is made to correlate the impact sensitivity of the three solids with their electronic structure. Band gap is an important parameter to characterize the electronic structure of solids. Table 3 presents the energy gaps between valence and conduction bands for crystalline MATB, DATB, and TATB. This

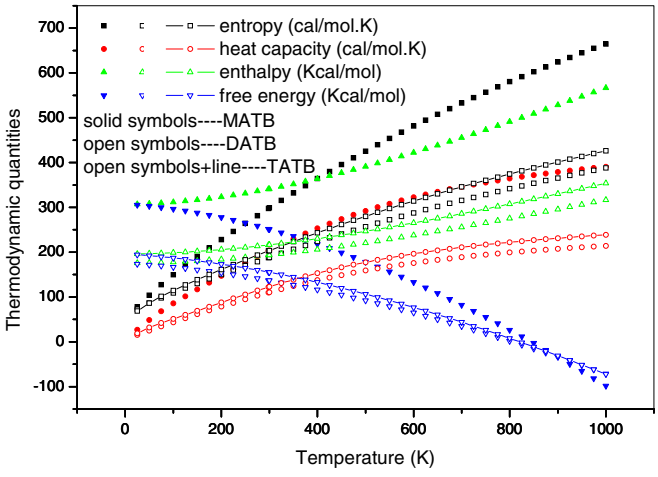

Fig. 6. Thermodynamic properties of crystalline MATB, DATB, and TATB as a function of temperature.

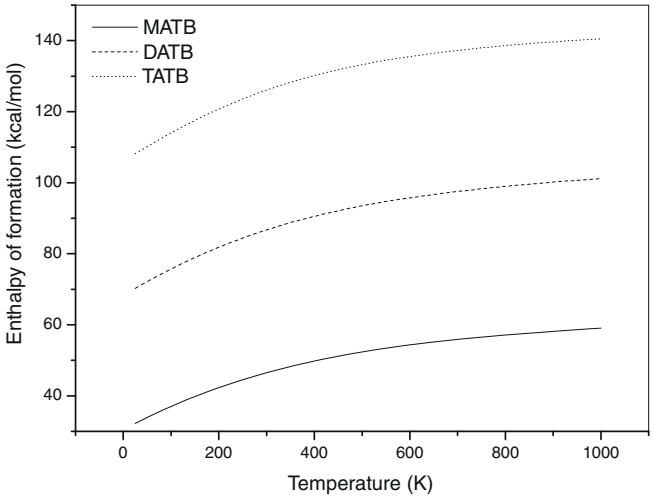

Fig. 7. Enthalpy of formation for crystalline MATB, DATB, and TATB as a function of temperature.

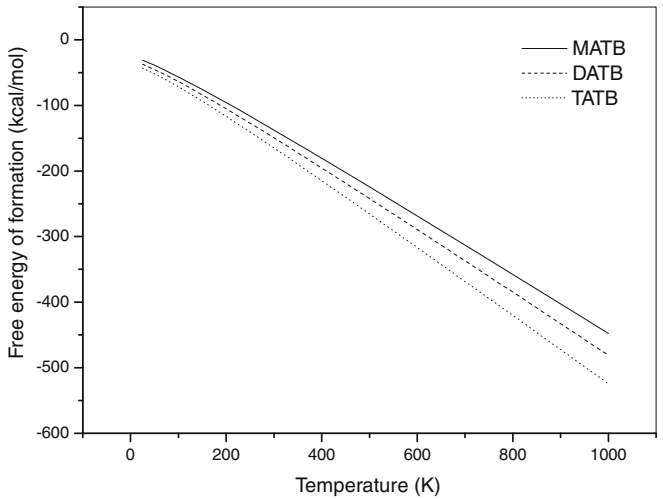

Fig. 8. Free energy of formation for crystalline MATB, DATB, and TATB as a function of temperature.

Table 3
Experimental impact sensitivity H_{50} (cm) and calculated band gap for crystalline MATB, DATB, and TATB.

	MATB	DATB	TATB [35]
Impact sensitivity H_{50} (cm) [34]	177	320	490
Sensitive order	Most sensitive	Sensitive	Least sensitive
Band gap (eV)	1.89	2.00	2.37

shows that the band gap increases in the sequence of MATB, DATB, and TATB, while their experimental impact sensitivity (shown in Table 3) decreases in the following order: MATB > DATB > TATB [34,35]. Therefore, there is a relationship between the band gap and impact sensitivity for the three solids. A possible explanation may be that the smaller the band gap is, the easier the electron transfers from the valence band to the conduction band, and the more the solid becomes decomposed and exploded. In the previous studies [36,37], a "principle of the easiest transition" (PET) was put forward to investigate the relationship between the band gap and impact sensitivity for the metal azides. Although these calculations are performed at the semiempirical discrete variational X_α (DV–X_α) and extended Hückel-crystal orbital (EH–CO) levels, the results have shown that their band gap could be correlated with their explosive characters. Our recent reports on the heavy-metal azides [38] and the four HMX [31] and hexanitrohexaazaisowurtzitane (CL-20) [39] polymorphs within the framework of periodic DFT have also confirmed the relationship between the band gap and impact sensitivity. Gilman [40,41] has emphasized the role of HOMO–LUMO (highest occupied molecular orbital-lowest unoccupied molecular orbital) gap closure in the explosion of molecules suffering shear strain. Further reports [42,43] on the excitonic mechanism of detonation initiation show that the pressure inside the impact wave front reduces the band gap between valence and conducting bands and promotes the HOMO–LUMO transition within a molecule. Although these studies have suggested that the HOMO–LUMO gap in molecules suffering shear strain, impact wave, or distortion relates directly to the sensitivity, they further support our conclusion here that there is the relationship between the band gap and impact sensitivity.

4. Conclusions

In this study, we have performed a comparative DFT study of the electronic structure and thermodynamic properties of crystalline MATB, DATB, and TATB in the local density approximation. An analysis of electronic structure shows that the C–NO_2 bonds in the three solids are easier to be broken in the thermal decomposition than the C–NH_2 bonds. The calculated thermodynamic properties show that the order of their thermodynamic stability is TATB > DATB > MATB and their decomposition reactions are favorable under high temperature. Finally, an attempt is made to correlate the impact sensitivity of the three solids with their band gap. The result shows that there is the relationship between the band gap and impact sensitivity.

Acknowledgements

This work was partly supported by the National Natural Science Foundation of China (Grant No. 10576016), the "973" Project, and the Project-sponsored by the Scientific Research Foundation for the Returned Overseas Chinese Scholars, State Education Ministry.

References

[1] J. Kohler, R. Meyer, Explosives, VCH, New York, 2007.
[2] J. Akhaven, The Chemistry of Explosives, Royal Society of Chemistry, Cambridge, UK, 1998.
[3] H.M. Xiao, Molecular Orbital Theory for Nitro Compounds, National Defence Industry Press, Beijing, 1993.
[4] H.M. Xiao, Z.Y. Wang, J.M. Yao, Acta Chim. Sinica 43 (1985) 14.
[5] T.B. Brill, K.J. James, J. Phys. Chem. 97 (1993) 8752.
[6] K.K. Baldridge, J.S. Siegel, J. Am. Chem. Soc. 115 (1993) 10782.
[7] A.B. Kunz, Phys. Rev. B 53 (1996) 9733.
[8] T.D. Sewell, AIP Conf. Proc. 429 (1997) 269.
[9] H.M. Xiao, J.F. Fan, Z.M. Gu, H.S. Dong, Chem. Phys. 226 (1998) 15.
[10] M.R. Manaa, R.H. Gee, L.E. Fried, J. Phys. Chem. A 106 (2002) 8806.
[11] G.F. Ji, H.M. Xiao, H.S. Dong, Acta Chim. Sinica 60 (2002) 1209.
[12] G.F. Ji, H.M. Xiao, X.H. Ju, H.S. Dong, Acta Chim. Sinica 61 (2003) 1186.
[13] S.D. McGrane, A.P. Shreve, J. Chem. Phys. 119 (2003) 5834.
[14] H.J. Song, H.M. Xiao, H.S. Dong, Acta Chim. Sinica 65 (2007) 1101.
[15] H. Liu, J.J. Zhao, Z.Z. Gong, W. Zheng, J.G. Du, G.F. Ji, D.Q. Wei, J. At. Mol. Phys. 24 (2007) 291 (in Chinese).
[16] D.D. Dlott, M.D. Fayer, J. Chem. Phys. 92 (1990) 3798.
[17] A. Tokmanoff, M.D. Fayer, D.D. Dlott, J. Phys. Chem. 97 (1993) 1901.
[18] C.M. Tarver, J. Phys. Chem. A 101 (1997) 4845.
[19] M.D. Segall, P.J.D. Lindan, M.J. Probert, C.J. Pickard, P.J. Hasnip, S.J. Clark, M.C. Payne, J. Phys. Condens. Matter. 14 (2002) 2717.
[20] D. Vanderbilt, Phys. Rev. B 41 (1990) 7892.
[21] G. Kresse, J. Furthmüller, Phys. Rev. B 54 (1996) 11169.
[22] R. Fletcher, Practical Methods of Optimization, vol. 1, Wiley, New York, 1980.
[23] D.M. Ceperley, B.J. Alder, Phys. Rev. Lett. 45 (1980) 566.
[24] J.P. Perdew, A. Zunger, Phys. Rev. B 23 (1981) 5048.
[25] J.R. Holden, C. Dickinson, C.M. Bock, J. Phys. Chem. 76 (1972) 3597.
[26] J.R. Holden, Acta Crystallogr. 22 (1967) 545.
[27] H.H. Cady, A.C. Larson, Acta Crystallogr. 18 (1965) 485.
[28] D. Sanchez-Portal, E. Artacho, J.M. Soler, Solid State Commun. 95 (1995) 685.
[29] M.D. Segall, R. Shah, C.J. Pickard, M.C. Payne, Phys. Rev. B 54 (1996) 16317.
[30] X. Gonze, Phys. Rev. B 55 (1997) 10337.
[31] W.H. Zhu, J.J. Xiao, G.F. Ji, F. Zhao, H.M. Xiao, J. Phys. Chem. B 111 (2007) 12715.
[32] J.P. Perdew, K. Burke, M. Ernzerhof, Phys. Rev. Lett. 77 (1996) 3865.
[33] J.P. Perdew, J.A. Chevary, S.H. Vosko, K.A. Jackson, M.R. Pederson, D.J. Singh, C. Fiolhais, Phys. Rev. B 46 (1992) 6671.
[34] M.J. Kamlet, H.G. Adolph, Propellants Explos. 4 (1979) 30.
[35] C.B. Storm, J.R. Stine, J.F. Kramer, in: S. Bulusu (Ed.), Chemistry and Physics of Energetic Materials, Kluwer Academic Publishers, Dordrecht, The Netherlands, 1990.
[36] H.-M. Xiao, Y.-F. Li, Sci. China B 38 (1995) 538.
[37] H.-M. Xiao, Y.-F. Li, Banding and Electronic Structures of Metal azides, Science Press, Beijing, 1996. p. 88. (in Chinese).
[38] W.H. Zhu, H.M. Xiao, J. Comput. Chem. 29 (2008) 176.
[39] X.J. Xu, W.H. Zhu, H.M. Xiao, J. Phys. Chem. B 111 (2007) 2090.
[40] J.J. Gilman, Philos. Mag. Lett. 77 (1998) 79.
[41] J.J. Gilman, Philos. Mag. B 67 (1993) 207.
[42] T. Luty, P. Ordon, C.J. Eckhardt, J. Chem. Phys. 117 (2002) 1775.
[43] M.M. Kuklja, E.V. Stefanovich, A.B. Kunz, J. Chem. Phys. 112 (2000) 3417.